Effects of Light Intensity on the Steady-State Fluorescence Quenching Kinetics

Mino Yang, Sangyoub Lee*, Kook Joe Shin*, and Kwang Yul Choo†

Department of Chemistry, Seoul National University, Seoul 151-742

Duckhwan Lee

Department of Chemistry, Sogang University, Seoul 121-742. *Received March 20, 1991*

Effects of light intensity on the steady-state fluorescence quenching kinetics are examined for general cases where the bimolecular quenching can occur *via* long-range energy transfer processes and the potential of mean force between the energy donor and acceptor molecules is not negligible. Approximate analytic expressions are derived for the steady-state quenching rate constant and for the ratio of the steady-state intensity of unquenched to quenched fluorescence. The analytic results are compared with the exact results obtained from numerical analysis and the results of conventional theories.

Introduction

There have been many studies of the quenching of fluorescence from both experimental[1-10] and theoretical perspectives[11-19]. In some experiments[2-8], fluorescent molecules are produced by a light pulse of short duration and the decay of fluorescence intensity from the sample is followed as a function of time. In other experiments[1,2,9,10], the effects of quencher molecules on the steady-state intensity of fluorescence stimulated by an illumination of constant intensity are examined. The present theory addresses the latter class of experiments although the basic framework is also relevant to the former[20].

When the concentration of fluorescent molecules is much smaller than that of quencher molecules, a quencher molecule may be able to dispose of the energy it received from a fluorescent molecule before it has an opportunity to quench again. If this is the case, the fluorescence quenching kinetics can be described by the following reaction scheme[11]:

$$D+h\nu_e \xrightarrow{F} D^* \text{ (excitation of fluorophors)} \quad (1.1)$$

$$D^* \xrightarrow{k_F} D+h\nu_F \text{ (fluorescence)} \quad (1.2)$$

$$D^* \xrightarrow{k_{NR}} D \text{ (nonradiative unimolecular decay)} \quad (1.3)$$

$$D^*+A \xrightarrow{k_Q} D+A \text{ (bimolecular quenching)} \quad (1.4)$$

In these equations, F, k_F, k_{NR}, and k_Q represent the rate constants of the respective processes. k_F and k_{NR} may be considered to be independent of time, and their sum, denoted hereafter by k_S, can be determined experimentally as the inverse of the fluorescent life time τ_o in the absence of quencher; that is,

$$k_F+k_{NR}\equiv k_S=\tau_o^{-1} \quad (1.5)$$

F in Eq. (1.1), denoting the transition probability per unit time, depends on the intensity of radiation and thus varies with time in general. The bimolecular quenching rate coefficient k_Q in Eq. (1.4) depends on the distribution of the quencher molecules A around D^*. When the relative diffusion between D^* and A is slow, this distribution deviates from the equilibrium one and varies with time, and so does the bimolecular quenching coefficient k_Q.

The time-dependence of the concentration (number density) of D^* molecules may then obey the phenomenological rate law:

$$\frac{d}{dt}[D^*]=-k_S[D^*]+F(t)[D]-k_Q(t)[D^*]C_A^\circ \quad (1.6)$$

where $[D]$ and $[D^*]$ denote the number densities of D and D^* molecules at time t, respectively, and C_A° is the number density of A molecules that is essentially constant in time. By solving this differential equation, we obtain

$$[D^*]=C_D^\circ \int_0^t d\tau F(\tau) \exp\left[-k_S(t-\tau)-\int_\tau^t d\tau_1 F(\tau_1) - C_A^\circ \int_\tau^t d\tau_1 k_Q(\tau_1)\right] \quad (1.7)$$

where C_D° is the total number density of D molecules. That is $C_D^\circ=[D^*]+[D]$.

The time-dependece of $[D^*]$ may also be expressed as

$$[D^*]=\int_0^t d\tau F(\tau)[D]G(\tau, t) \quad (1.8)$$

Here, $F(\tau)[D]d\tau$ gives number of D^* molecules generated in a unit volume between times τ and $\tau+d\tau$, and $G(\tau, t)$ denotes the probability that a D^* molecule excited at time τ remains in the excited state at time t. This is an exact expression. In conventional theories[11], however, it is assumed that each D^* molecule which has been just excited is surrounded by an equilibrium distribution of A molecules and that the A molecule distribution around each D^* follows the same time evolution thereafter. This means that the decay probability of D^* depends only on the time elapsed after excitation regardless of when the excitation occurred. That is, $G(\tau, t)$ in Eq. (1.8) is approximated as

$$G(\tau, t)\approx G(t-\tau)=\exp\left[-k_S(t-\tau)-C_A^\circ \int_0^{t-\tau} d\tau_1 k_Q^{CS}(\tau_1)\right] \quad (1.9)$$

†Deceased January 24, 1991.

where $k_Q^{CS}(\tau_1)$ is the quenching rate coefficient obtained for the initial condition that each D^* molecule created at $\tau_1=0$ is surrounded by an equilibrium distribution of A molecules; see Eq. (3.62) below. Consequently, it is different from $k_Q(\tau_1)$ in Eq. (1.7).

In most analyses of experimental data[1-8], one goes one step further by assuming that $[D]\gg[D^*]$ and thus $[D]$ remains nearly constant in time; that is, $[D]\approx C_D^0$. Then Eq. (1.8) gives

$$[D^*]=C_D^0\int_0^t d\tau\, F(\tau)\exp\left[-k_S(t-\tau)-C_A^0\int_0^{t-\tau}d\tau_1\, k_Q^{CS}(\tau_1)\right] \tag{1.10}$$

Comparison of Eq. (1.10) with Eq. (1.7) shows clearly that its validity is limited by the condition that the intensity of illumination which excites D molecules ought to be weak to ensure that $[D^*]\ll[D]$.

The assumption that each D^* molecule which has been just excited is surrounded by an equilibrium distribution of A molecules fails when the duration of light pulse is not so short compared to the life time of D^* molecules. For instance, D^* molecules which were recently quenched but reexcited shortly will see, on the average, more A molecules in their vicinity than the equilibrium distribution that is presupposed in conventional theories. For such D^* molecules, the decay law would be different from that given by Eq. (1.9). The opportunity of repeated excitations grows with increases in the intensity and time width of light pulse and also with increase in the quencher concentration, and the conventional theories of fluorescence quenching are expected to break down in such situations.

In a previous work[20], we proposed a general theoretical framework that is relatively rigorous and, nevertheless, computationally viable approach to this complicated problem, which is based on a hierarchical system of many-body Smoluchowski equations for the reactant molecules[21]. The formalism is free of the above mentioned limitations of conventional theories. We then applied the theory to treat the steady-state fluorescence quenching kinetics. For the simplest case where the bimolecular quenching occurs only upon contact of D^* and A moledules and the potential of mean force between them has a negligible effect, exact expressions were obtained for the steady-state quenching rate coefficient and for the ratio of the steady-state fluorescence intensity in the absence (I_0) and in the presence (I) of quencher.

The purpose of the present work is to extend the previous treatment[20] to the general cases where the bimolecular quenching may also occur *via* long-range energy transfer processes and the potential of mean force is not negligible. We obtain some approximate analytic expressions for the steady-state quenching rate coefficient and for the ratio I_0/I. The present theory predicts a complicated nonlinear dependence of I_0/I on quencher concentration C_A^0. The Stern-Volmer coefficient K_{SV}, which is defined by[2,14]

$$K_{SV}=(I_0/I-1)/C_A^0 \tag{1.11}$$

depends on C_A^0 and the intensity of light that excites the fluorophor as well as on other parameters that characterize the dynamics of the fluorophor and quencher in a given solution. The approximate analytic results are then compared with the exact results obtained from numerical analysis and the results obtained from the conventional Smoluchowski theory[11]. It is seen that the conventional theory breaks down when the light intensity is very high and when the quencher concentration is high.

The Many-Body Smoluchowski Equation Approach

In the previous work[20], starting from a hierarchical system of many-body Smoluchowski equations for the reactant distribution functions, we were able to show that the time-dependent bimolecular quenching rate coefficient $k_Q(t)$ appearing in the rate law, Eq. (1.6), can be evaluated from the following expression:

$$k_Q(t)=\int dr\; 4\pi r^2 S(r)\rho_{AD^*}(r,\,t) \tag{2.1}$$

Here, $S(r)$ is the sink function which describes the rate of quenching of a D^* molecule when there is an A molecule at the separation of r. $\rho_{AD^*}(r,\,t)$ is the nonequilibrium pair distribution function; *i.e.*, $4\pi r^2 dr\rho_{AD^*}(r,\,t)C_A^0$ is the number of A molecules located, on average, in a spherical shell of thickness dr at a distance r from a D^* molecule at time t.

We also showed that under irradiation for $t>0$ $\rho_{AD^*}(r,\,t)$ evolves in time according to the kinetic equation,

$$\frac{\partial}{\partial t}\rho_{AD^*}(r,\,t)=L_{D^*A}^0(r,\,t)-S(r)\rho_{AD^*}(r,\,t)+F(t)\frac{[D]}{[D^*]}[\rho_{AD}(r,\,t)-\rho_{AD^*}(r,\,t)] \qquad (t>0) \tag{2.2}$$

Here, $L_{D^*A}^0$ is the Smoluchowski operator for the relative motion of D^* and A and its explicit form is given by

$$L_{D^*A}^0=\left(\frac{\partial}{\partial r}+\frac{2}{r}\right)d_{AD^*}(r)\left[\frac{\partial}{\partial r}+\beta\frac{\partial}{\partial r}U_{AD^*}(r)\right] \tag{2.3}$$

where $d_{AD^*}(r)$ is the diffusion coefficient, which depends on r if the hydrodynamic interaction between D^* and A is to be included, and $U_{AD^*}(r)$ is the potential of mean force. $\beta=1/k_BT$ with the Boltzmann constant k_B and the absolute temperature T. If $U_{AD^*}(r)$ has a very steep potential wall at $r=\sigma$, $\rho_{AD^*}(r,\,t)$ must satisfy the reflecting boundary condition,

$$\left\{d_{AD^*}(r)\left[\frac{\partial}{\partial r}+\beta\frac{\partial}{\partial r}U_{AD^*}(r)\right]\rho_{AD^*}(r,\,t)\right\}_{r=\sigma}=0 \tag{2.4}$$

On the other hand, as r goes to infinity, $\rho_{AD^*}(r,\,t)$ approaces unity:

$$\lim_{r\to\infty}\rho_{AD^*}(r,\,t)=1 \tag{2.5}$$

The initial condition for $\rho_{AD^*}(r,\,t)$ that corresponds to usual experimental conditions is

$$\rho_{AD^*}(r,\,t=0)=\exp[-\beta U_{AD^*}(r)] \tag{2.6}$$

The kinetic equation for $\rho_{AD^*}(r,\,t)$ in Eq. (2.2) involves another nonequilibrium pair distribution function $\rho_{AD}(r,\,t)$, which gives the correlation in the distribution of A and ground state D molecules. The kinetic equation governing

the evolution of $\rho_{AD}(r, t)$ is given by

$$\frac{\partial}{\partial t}\rho_{AD}(r,t)=L^{\circ}_{DA}\,\rho_{AD}(r,\ t)+S(r)\frac{[D^*]}{[D]}\,\rho_{AD^*}(r,\ t)$$
$$+\frac{[D^*]}{[D]}\,[k_S+k_Q(t)C^{\circ}_A][\rho_{AD^*}(r,\ t)-\rho_{AD}(r,\ t)]$$
$$(t>0) \tag{2.7}$$

The Smoluchowski operator L°_{DA} for the relative motion of D and A has the same structure as $L^{\circ}_{D^*A}$ in Eq. (2.3), and the boundary and initial conditions for $\rho_{DA^*}(r, t)$ are also similar to those for $\rho_{AD^*}(r, t)$ in Eqs. (2.4)-(2.6).

Eqs. (2.1), (2.2), and (2.7) together with Eq. (1.6) constitute the set of integro-differential equations to be solved for the four unknowns, $[D^*]$, $k_Q(t)$, $\rho_{AD^*}(r, t)$, and $\rho_{AD}(r, t)$. We assume that k_S, F, and $S(r)$ are known from quantum mechanical caluclations or independent experiments.

However, if the potential of mean force between D^* and A does not differ much from that between D and A [*i.e.*, if $U_{AD^*}(r)\cong U_{AD}(r)$], the problem can be simplified greatly. In such cases, we have

$$[D^*]\rho_{AD^*}(r,\ t)+[D]\rho_{AD}(r,\ t)=C^{\circ}_D g^{(2)}(r) \tag{2.8}$$

where $g^{(2)}(r)$ is the equilibrium radial distribution function between D and A,

$$g^{(2)}(r)=\exp[-\beta U_{AD}(r)]\cong\exp[-\beta U_{AD^*}(r)] \tag{2.9}$$

With Eq. (2.8), the kinetic equation for $\rho_{AD^*}(r, t)$, Eq. (2.2), becomes decoupled from that for $\rho_{AD}(r, t)$, Eq. (2.7), to give

$$\frac{\partial}{\partial t}\rho_{AD^*}(r,\ t)=L^{\circ}_{D^*A}\,\rho_{AD^*}(r,\ t)-S(r)\rho_{AD^*}(r,\ t)$$
$$+\{F(t)C^{\circ}_D/[D^*]\}\,[g^{(2)}(r)-\rho_{AD^*}(r,\ t)]$$
$$(t>0) \tag{2.10}$$

Hence, only this equation together with Eqs. (1.6) and (2.1) has to be solved to obtain reaction kinetic informations. Hereafter, we will restrict our discussion to this situation.

Steady-State Fluorescence Quenching Kinetics

When the external radiation which excites the D molecules has constant intensity, a steady state is attained at long times. For this steady-state, $d[D^*]/dt=0$ and $\partial\rho_{AD^*}(r, t)/\partial t=0$. Therefore, the equations we have to solve, *i.e.* Eqs. (1.6), (2.1) and (2.10), become respectively

$$\gamma_s\equiv FC^{\circ}_D/[D^*]_s=k_S+F+k^s_Q C^{\circ}_A \tag{3.1}$$

$$k^s_Q=\int d\mathbf{r}\,S(r)[g^{(2)}(r)+f_s(r)]=k^0_Q+\int d\mathbf{r}\,S(r)f_s(r) \tag{3.2}$$

and

$$[\gamma_s-L^{\circ}+S(r)]f_s(r)=-S(r)g^{(2)}(r) \tag{3.3}$$

Here, $[D^*]_s$ and k^s_Q denote the steady-state values of $[D^*]$ and $k_Q(t)$, respectively, and the subscript D^*A of $L^{\circ}_{D^*A}$ has been omitted for the brevity of notation. $f_s(r)$ denotes the deviation of $\rho_{AD^*}(r, t)$ from $g^{(2)}_{AD}(r)$ in the long-time limit. Note also that in Eq. (3.2) we introduced the equilibrium quenching rate constant k^0_Q, with is given by

$$k^0_Q=\int d\mathbf{r}\,S(r)g^{(2)}(r) \tag{3.4}$$

If the redistribution of reactant molecules by diffusion occurred rapidly so that the pair distribution between D^* and A were give by $g^{(2)}(r)$, k^0_Q would be the rate constant for the bimolecular quenching process.

Once γ_s, k^s_Q and $f_s(r)$ are determined from Eqs. (3.1)-(3.2), the ratio of the steady-state fluorescence intensity in the absence (I_o) and in the presence (I) of quencher can be calculated from the following equation:

$$I_o/I=[D^*]_s\,(C^{\circ}_A=0)/[D^*]_s\,(C^{\circ}_A\neq 0)$$
$$=\gamma_s(C^{\circ}_A\neq 0)/\gamma_s(C^{\circ}_A=0)$$
$$=1+k^s_Q C^{\circ}_A/(k_S+F) \tag{3.5}$$

A formal solution to Eq. (3.3) may be written as

$$f_s(r)=-\int d\mathbf{r}_o\ G_S(r,\ r_o,\ \gamma_s)\,S(r_o)\,g^{(2)}(r_o) \tag{3.6}$$

where the Green's function $G_S(r, r_o, \gamma_s)$ satisfies the differential equation,

$$[\gamma_s-L^{\circ}(r)+S(r)]\,G_S(r,\ r_o,\ \gamma_s)=\delta(r-r_o)/4\pi r^2_o \tag{3.7}$$

and the same boundary conditions as those for $f_s(r)$, *i.e.*,

$$\lim_{r\to\infty} G_S(r,\ r_o,\ \gamma_s)=0 \tag{3.8}$$

and

$$[d_{AD^*}(r)\Big(\frac{\partial}{\partial r}+\beta\frac{\partial}{\partial r}U_{AD^*}\Big)G_S(r,\ r_o,\ \gamma_s)]_{r=\sigma}=0 \tag{3.9}$$

The notation $L^{\circ}(r)$ in Eq. (3.7) denotes that it operates on the variable r. $G_s(r, r_o, \gamma_s)$ can be, in turn, expressed in terms of a simpler Green's function:

$$G_S(r,\ r_o,\ \gamma_s)=G(r,\ r_o,\ \gamma_s)-\int d\mathbf{r}_1\ G(r,\ r_1,\ \gamma_s)S(r_1)G_S(r_1,\ r_o,\ \gamma_s) \tag{3.10}$$

where the *reaction-free* Green's function $G(r, r_1, \gamma_s)$ governs the D^*-A pair dynamics in the absence of the energy transfer reactions. It satisfies the differential equation.

$$[\gamma_s-L^{\circ}(r)]\,G(r,\ r_1,\ \gamma_s)=\delta(r-r_1)/4\pi r^2_1 \tag{3.11}$$

and the same boundary condition as $G_S(r, r_o, \gamma_s)$.

Contact Quenching

Suppose that the quenching reaction can occur only when the D^* and A molecules are brought into contact. In this case the sink function $S(r)$ may by modeled as a delta-function[22]:

$$S(r)=\frac{k^{s\,0}_Q}{g^{(2)}(\sigma)}\cdot\frac{\delta(r-\sigma)}{4\pi\sigma^2}\equiv\kappa\,\delta(r-\sigma)/4\pi\sigma^2 \tag{3.12}$$

where $\kappa=k^{s\,0}_Q/g^{(2)}(\sigma)$. From Eq. (3.10), we then have

$$G_S(r,\ r_o,\ \gamma_s)=G(r,\ r_o,\ \gamma_s)-\kappa G(r,\ \sigma,\ \gamma_s)G(\sigma,\ r_o,\ \gamma_s)$$
$$/[1+\kappa G(\sigma,\ \sigma,\ \gamma_s)] \tag{3.13}$$

and from Eq. (3.6)

$$f_s(r)=-k^0_Q G(r,\ \sigma,\ \gamma_s)/[1+\kappa G(\sigma,\ \sigma,\ \gamma_s)] \tag{3.14}$$

Substituting this expression for $f_s(r)$ in Eq. (3.2), we obtain the steady-state quenching rate constant,

$$k_Q^s = k_Q^a/[1+\kappa G(\sigma, \sigma, \gamma_s)] \tag{3.15}$$

which is obviously smaller than the equilibrium rate constant k_Q^a. Finally, putting this expression for k_Q^s into Eq. (3.1), we obtain an algebraic equation for γ_s:

$$\gamma_s = k_S + F + C_A^\circ k_Q^a/[1+\kappa G(\sigma, \sigma, \gamma_s)] \tag{3.16}$$

By solving this equation for γ_s, we can calculate the steady-state quenching rate constant from Eq. (3.15) and in turn the ratio $I_\circ/I$ from Eq. (3.5).

Hard sphere model with $U_{AD^*}(r)=0$ for $r\geq\sigma$. For simplicity, we assume that the potential of mean force $U_{AD^*}(r)$ vanishes $r\geq\sigma$ but goes to infinity for $r<\sigma$. We also assume that the hydrodynamic interaction between D^* and A is negligible so that $d_{AD^*}(r)=D_A+D_{D^*}\equiv D=$constant. In this simplest case, the Green's function $G(r, r_1, \gamma_s)$ can be readily obtained:

$$G(r, r_1, \gamma_s)=\frac{1}{4\pi D r r_1}\left\{\frac{1}{2\alpha}\left[e^{-\alpha|r-r_1|}-e^{-\alpha(r+r_1-2\sigma)}\right]+\frac{\sigma}{1+\alpha\sigma}e^{-\alpha(r+r_1-2\sigma)}\right\} \tag{3.17}$$

where $\alpha\equiv(\gamma_s/D)^{1/2}$. The equation for γ_s is then given by

$$\gamma_s = k_S + F + C_A^\circ k_Q^a/[1+k_Q^a/k_D(1+\sigma\gamma_s^{1/2}/D^{1/2})] \tag{3.18}$$

where $k_D\equiv 4\pi\sigma D$. It was shown[20] that the root of Eq. (3.18) is given by

$$\gamma_s = X_2(k_S + F + k_Q^a C_A^\circ) \tag{3.19}$$

Expression for the coefficient X_2, which is less than unity, is rather complicated and is given by

$$X_2 = 2(-Q)^{1/2}\cos[(\Theta-2\pi)/3]-b_1/3 \tag{3.20}$$

where

$$\cos\Theta = R(-Q^3)^{-1/2};\quad Q=(3b_2-b_1^2)/9;\quad R=(9b_1b_2-27b_3-2b_1^3)/54;$$

$$b_1\equiv -(2+B^2/C^2);\quad b_2\equiv 1+2B(B-A)/C^2;$$

$$b_3\equiv -[(A-B)/C]^2;$$

$$A=\left(\frac{k_Q^s C_A^\circ}{\gamma_{eq}}\right)\left(\frac{k_Q^a}{k_D}\right);\quad B=1+\left(\frac{k_Q^a}{k_D}\right);\quad C=\left(\frac{\gamma_{eq}\sigma^2}{D}\right)^{1/2};$$

$$\gamma_{eq}\equiv k_S+F+k_Q^a C_A^\circ$$

X_2 depends on F on the quencher concentration C_A° as well as on other parameters that characterize the dynamics of D and A in a given solution, and its value approaches unity as $C_A^\circ\to 0$:

$$X_2 = 1-\left\{\frac{(k_Q^a/k_D)[k_Q^a/(k_S+F)]}{1+(k_Q^a/k_D)+[(k_S+F)\sigma^2/D]^{1/2}}\right\}C_A^\circ \quad (\text{when } C_A^\circ\to 0) \tag{3.21}$$

With the expression for γ_s in Eq. (3.19), the steady-state quenching rate constant k_Q^s in Eq. (3.15) is now explicitly given by

$$k_Q^s = k_Q^a/\{1+(k_Q^a/k_D)[1+(\gamma_s/D)^{1/2}\sigma]^{-1}\} \tag{3.22}$$

When this expression for k_Q^s is used in Eq. (3.5), the ratio $I_\circ/I$ can also be determined. Another expression for $I_\circ/I$ can be otained directly from Eq. (3.19) by noting that the value of X_2 becoms unity as $C_A^\circ\to 0$:

$$I_\circ/I=\gamma_s(C_A^\circ\neq 0)/\gamma_s(C_A^\circ=0)=X_2[1+k_Q^a C_A^\circ/(k_S+F)] \tag{3.23}$$

In the low quencher concentration limit, X_2 is given by Eq. (3.21) and thus Eq. (3.23) becomes

$$I_\circ/I = 1+K_{SV}^\circ C_A^\circ \quad (\text{when } C_A^\circ\to 0) \tag{3.24}$$

where the infinite dilution Stern-Volmer coefficient K_{SV}° is given by

$$K_{SV}^\circ = \lim_{C_A^\circ\to 0}(I_\circ/I-1)/C_A^\circ = \left(\frac{k_Q^a}{k_S+F}\right)\left\{1-\frac{k_Q^a/k_D}{1+(k_Q^a/k_D)+[(k_S+F)\sigma^2/D]^{1/2}}\right\} \tag{3.25}$$

Hard sphere model with $U_{AD^*}(r)\neq 0$ for $r\geq\sigma$. We now consider the case where the effect of potential of mean force is not negligible, *i.e.* $U_{AD^*}(r)\neq 0$ for $r\geq\sigma$, but the hydrodynamic interaction is still negligible, *i.e.* $d_{AD^*}(r)=D=$ constant. To level off the variation of the Green's function $G(r, r_1, \gamma_s)$ due to the Boltzmann factor $\exp[-\beta U_{AD^*}(r)]$ to some extent and to get a differential equation in a simple form, we introduce the following transformations[23]:

$$g(y, y_1, s)=\frac{4\pi D r r_1}{\sigma}\exp\left\{\frac{\beta}{2}[U(r)-U(r_1)]\right\}G(r, r_1, \gamma_s) \tag{3.26}$$

where $y\equiv(r/\sigma)-1$, $y_1\equiv(r_1/\sigma)-1$ and $s\equiv(\sigma^2/D)\gamma_s$. The subscript AD^* of $U_{AD^*}(r)$ has been omitted for the brevity of notation. The differential equation for $g(y, y_1, s)$ is given by

$$\left\{s-\left[\frac{\partial^2}{\partial y^2}+V(y)\right]\right\}g(y, y_1, s)=\delta(y-y_1) \tag{3.27}$$

where

$$V(y)\equiv \mathcal{V}(r(y))/(y+1)^2$$

with

$$\mathcal{V}(r)=r^2\left[\frac{1}{2}\frac{\partial^2(\beta U)}{\partial r^2}-\frac{1}{4}\left(\frac{\partial(\beta U)}{\partial r}\right)^2+\frac{1}{r}\frac{\partial(\beta U)}{\partial r}\right]$$

Boundary conditions for $g(y, y_1, s)$ are

$$\lim_{y\to\infty} g(y, y_1, s)=0 \tag{3.28}$$

$$\left[\frac{\partial g}{\partial y}+\left(\frac{1}{2}\frac{\partial(\beta U)}{\partial y}-1\right)g\right]_{y=0}=0 \tag{3.29}$$

Again, $g(y, y_1, s)$ may be expressed in terms of a simpler Green's function:

$$g(y, y_1, s)=g_\circ(y, y_1, s)+\int_0^\infty dy_2\, g_\circ(y, y_2, s)V(y_2)g(y_2, y_1, s) \tag{3.30}$$

The *field-free* Green's function $g_\circ(y, y_2, s)$ satisfies the differential equation,

$$\left(s-\frac{\partial^2}{\partial y^2}\right)g_0(y,\ y_2,\ s)=\delta(y-y_2) \tag{3.31}$$

and the same boundary conditions as those for $g(y,\ y_1,\ s)$ in Eqs. (3.28) and (3.29). It is almost equivalent to the Green's function in Eq. (3.17):

$$g_0(y,\ y_2,\ s)=\frac{1}{2s^{1/2}}\{\exp[-s^{1/2}\mid y-y_2\mid]-\exp[-s^{1/2}(y+y_2)]\}$$

$$+\frac{1}{s^{1/2}+\eta}\exp[-s^{1/2}(y+y_2)] \tag{3.32}$$

where $\eta\equiv\left[1-\frac{1}{2}\ \frac{\partial(\beta U)}{\partial y}\right]_{y=0}$

A formal solution to the integral equation, Eq. (3.30), can be obtained by an iterative procedure. We can write

$$g(y,\ y_1,\ s)=\sum_{n=0}^{\infty}g^{(n)}(y,\ y_1,\ s) \tag{3.33}$$

where

$$g^{(0)}(y,\ y_1,\ s)=g_0(y,\ y_1,\ s)$$

$$g^{(n)}(y,\ y_1,\ s)=\int_0^\infty dy_2\ g_0(y,\ y_2,\ s)V(y_2)g^{(n-1)}(y,\ y_1,\ s)\ \text{for}\ n\geq 1.$$

What we need is not the complete expression for $g(y,\ y_1,\ s)$ but its value at $y=0$:

$$g(0,\ y_1,\ s)=\sum_{n=0}^{\infty}g^{(n)}(0,\ y_1,\ s) \tag{3.34}$$

with

$$g^{(0)}(0,\ y_1,\ s)=g_0(0,\ y_1,\ s)=\exp[-s^{1/2}y_1]/(s^{1/2}+\eta) \tag{3.35}$$

and

$$g^{(n)}(0,\ y_1,\ s)=\int_0^\infty dy\,g_0(0,\ y,\ s)\ V(y)\ g^{(n-1)}(y,\ y_1,\ s)$$

$$(n\geq 1) \tag{3.36}$$

When $V(y)$ is short-ranged, the main contribution to the integral in Eq. (3.36) comes from the values of y near zero. We may then approximate $g^{(n-1)}(y,\ y_1,\ s)$ as

$$g^{(n-1)}(y,\ y_1,\ s)\cong g^{(n-1)}(0,\ y_1,\ s)$$

$$+\left[\frac{\partial}{\partial y}g^{(n-1)}(y,\ y_1,\ s)\right]_{y=0}y \tag{3.37}$$

The derivative in the second term on the right hand side can be related to $g^{(n-1)}(0,\ y_1,\ s)$ by the inner boundary condition to give

$$\left[\frac{\partial}{\partial y}g^{(n-1)}(y,\ y_1,\ s)\right]_{y=0}=\eta g^{(n-1)}(0,\ y_1,\ s) \tag{3.38}$$

Substitution of Eqs. (3.37) and (3.38) into Eq. (3.36) yields

$$g^{(n)}(0,\ y_1,\ s)\cong[\zeta(s)]^n g_0(0,\ y_1,\ s) \tag{3.39}$$

where

$$\zeta(s)\equiv\int_0^\infty dy\,g_0(0,\ y,\ s)V(y)(1+\eta y) \tag{3.40}$$

From Eqs. (3.34), (3.35) and (3.39), we therefore obtain

$$g(0,\ y_1,\ s)\cong\{\sum_{n=0}^{\infty}[\zeta(s)]^n\}\,g_0(0,\ y_1,\ s)$$

$$=\frac{\exp[-s^{1/2}y_1]}{s^{1/2}+\eta}\cdot\frac{1}{1-\zeta(s)} \tag{3.41}$$

if $\mid\zeta(s)\mid<1$, and

$$G(\sigma,\ r_1,\ \gamma_s)\cong g(0,\ y_1,\ s)\exp\{-\frac{\beta}{2}[U(\sigma)-U(r_1)]\}/(4\pi Dr_1)$$

$$=[4\pi Dr_1(s^{1/2}+\eta)(1-\zeta(s))]^{-1}\exp\{-\frac{\beta}{2}[U(\sigma)-U(r_1)]\}$$

$$\times\exp[-s^{1/2}y_1] \tag{3.42}$$

Finally, putting this expression for $G(\sigma,\ \sigma,\ \gamma_s)$ into Eq. (3.16), we obtain an algebraic equation for γ_s:

$$\gamma_s=k_s+F+C_A^0k_Q^0/\{1+k_Q^0/[(4\pi\sigma D)g^{(2)}(\sigma)(s^{1/2}+\eta)(1-\zeta(s))]\} \tag{3.43}$$

By solving this equation numerically, we can in turn calculate $[D^*]_s$ from Eq. (3.1) and the ratio I_0/I.

Long-Range Energy Transfer

We now consider the case where $S(r)$ contains a long-range interaction term $S_L(r)$, that is,

$$S(r)=\kappa_C\delta(r-\sigma)/4\pi\sigma^2+S_L(r) \tag{3.44}$$

where κ_C measures the quenching rate at contact radius. In this case, the steady-state quenching rate constant in Eq. (3.2) can be expressed as

$$k_Q^s=k_Q^0+\kappa_C f_s(\sigma)+\int dr S_L(r)\,f_s(r) \tag{3.45}$$

$f_s(r)$ in Eq. (3.6) is in turn given by

$$f_s(r)=-\kappa_C g^{(2)}(\sigma)\ G_S(r,\ \sigma,\ \gamma_s)$$

$$-\int dr_0\ G_S(r,\ r_0,\ \gamma_s)S_L(r_0)g^{(2)}(r_0) \tag{3.46}$$

If $S_L(r)$ is not too long-ranged, the integral appearing appearing in Eq. (3.45) may be approximated as follows:

$$\int dr S_L(r)f_s(r)\cong\int dr S_L(r)\{f_s(\sigma)+\left[\frac{\partial f_s(r)}{\partial r}\right]_{r=\sigma}(r-\sigma)\} \tag{3.47}$$

The boundary condition for $f_s(r)$ at $r=\sigma$ gives the relation

$$\left[\frac{\partial f_s(r)}{\partial r}\right]_{r=\sigma}=-\psi f_s(\sigma) \tag{3.48}$$

with $\psi=\beta\left[\frac{\partial}{\partial r}U_{AD^*}(r)\right]_{r=\sigma}$. We can then approximate k_Q^s as

$$k_Q^S=k_Q^{eq}+(\kappa_C+\kappa_L)f_s(\sigma) \tag{3.49}$$

where

$$\kappa_L=\int dr\,S_L(r)[1-(r-\sigma)\psi] \tag{3.50}$$

In deriving an expression for the *full* Green's function $G_s(r,\ r_0,\ \gamma_s)$, we isolate the influnce of contact quenching by introducing a *long-range-interaction-free* Gree's function $G_C(r,\ r_1,\ \gamma_s)$, which is a solution of differential equation

$$[\gamma_s - L^\circ(r) + \kappa_C\delta(r-\sigma)/4\pi\sigma^2]G_C(r, r_1, \gamma_s) = \delta(r-r_1)/4\pi r_1^2 \tag{3.51}$$

and satisfies the same boundary conditions as those for G_S in Eqs. (3.8) and (3.9). $G_s(r, r_o, \gamma_s)$, is then expressed as

$$G_s(r, r_o, \gamma_s) = G_C(r, r_o, \gamma_s) - \int dr_1 G_C(r, r_1, \gamma_s)S_L(r_1) \times G_S(r_1, r_o, \gamma_s) = \sum_{n=0}^{\infty} G_S^{(n)}(r, r_o, \gamma_s) \tag{3.52}$$

where

$$G_S^{(0)}(r, r_o, \gamma_s) = G_C(r, r_o, \gamma_s) \tag{3.53}$$

and for $n \geq 1$

$$G_S^{(n)}(r, r_o, \gamma_s) = -\int dr_1 G_C(r, r_1, \gamma_s)S_L(r_1)G_S^{(n-1)}(r_1, r_o, \gamma_s) \tag{3.54}$$

Again, for $S_L(r)$ that is not too long-ranged we make the following approximation:

$$\begin{aligned} G_S^{(n)}(r, r_o, \gamma_s) \cong & -\int dr_1 G_C(r, r_1, \gamma_S)S_L(r_1) \\ & \times [G_S^{(n-1)}(\sigma, r_o, \gamma_s) \\ & + [\frac{\partial}{\partial r_1} G_S^{(n-1)}(r_1, r_o, \gamma_s)]_{r_1=\sigma}(r_1-\sigma)] \\ = & -\int dr_1 G_C(r, r_1, \gamma_s)S_L(r_1)[1-(r_1-\sigma)\psi]G_s^{(n-1)}(\sigma, r_o, \gamma_s) \end{aligned} \tag{3.55}$$

where the second line has been obtained by assuming that the boundary condition, Eq. (3.9), holds for G_S at all orders of approximation given by the expansion in Eq. (3.52). The value of $G_S^{(n)}(r, r_o, \gamma_s)$ at $=\sigma$ is then given by

$$G_S^{(n)}(\sigma, r_o, \gamma_s) = (-1)^n [\xi(\gamma_s)]^n G_C(\gamma, r_o, \gamma_s) \tag{3.56}$$

where

$$\xi(\gamma_s) = \int dr_1 G_C(\sigma, r_1, \gamma_s) S_L(r_1)[1-(r_1-\sigma)\psi] \tag{3.57}$$

Substitution of Eqs. (3.53) and (3.56) into Eq. (3.52) gives an expression for $G_S(\sigma, r_o, \gamma_s)$ in the closed form:

$$G_S(\sigma, r_o, \gamma_s) = G_C(\sigma, r_o, \gamma_s)/[1+\xi(\gamma_s)] \tag{3.58}$$

if $|\xi(\gamma_s)| < 1$.

The long-range-interaction-free Gree's function $G_C(r, r_o, \gamma_s)$ is given by Eq. (3.13) with κ replace by κ_C and thus

$$G_C(\sigma, r_o, \gamma_s) = G(\sigma, r_o, \gamma_s)/[1+\kappa_C G(\sigma, \sigma, \gamma_s)] \tag{3.59}$$

where $G(r, r_o, \gamma_s)$ is the reaction-free Green's function obtained in the previous subsection, Eqs. (3.17) and (3.42)

First obtaining an expression for $f_s(\sigma)$ from Eqs. (3.46), (3.58) and (3.59) and then putting the resulting expression into Eq. (3.49), we finally have

$$k_Q^s = k_Q^a - (\kappa_C + \kappa_L) \times \left\{ \frac{\kappa_C g^{(2)}(\sigma)G(\sigma, \sigma, \gamma_s) + \int dr_o G(\sigma, r_o, \gamma_s)S_L(r_o)g^{(2)}(r_o)}{1+\kappa_C G(\sigma, \sigma, \gamma_s) + \int dr_o G(\sigma, r_o, \gamma_s)S_L(r_o)[1-(r_o-\sigma)\psi]} \right\} \tag{3.60}$$

When $S_L(r)=0$, we have $\kappa_L=0$ and $\kappa_C = k_Q^a/g^{(2)}(\sigma)$, and thus this expression for k_Q^s reduces to that given by Eq. (3.15). By solving the nonlinear algebraic equation for γ_s, obtained by substituting the above expression for k_Q^s into Eq. (3.1), we can calculate $[D^*]_s$ and thus the ratio I_o/I.

Relation to the Conventional Smoluchowski Approach

In most analyses of experimental data[1-8,11], the validity of Eq. (1.10) was taken for granted. This gives

$$I_o/I = k_S^{-1}\left\{ \int_0^\infty dt \exp\left[-k_S t - C_A^o \int_0^t d\tau\, k_Q^{CS}(\tau) \right] \right\}^{-1} \tag{3.61}$$

In the conventional Smoluchowski approach[11], the time-dependent quenching rate coefficient $k_Q^{CS}(\tau)$ in Eq. (3.61) is evaluated by

$$k_Q^{CS}(t) = \int dr\, S(r)\rho_{CS}(r, t) \tag{3.62}$$

Here, the nonequilibrium pair distribution function $\rho_{CS}(r, t)$ is the solution of

$$\frac{\partial}{\partial t}\rho_{CS}(r, t) = L^\circ(r)\rho_{CS}(r, t) - S(r)\rho_{CS}(r, t) \tag{3.63}$$

with the same boundary and initial conditions as given by Eqs. (2.4)-(2.6). For the simple case in which $S(r)$ is given by Eq. (3.12), $U_{AD^*}(r)=0$ for $r \geq \sigma$, and $d_{AD^*}(r) = D_A + D_{D^*} = D =$ constant, one can find an explicit expression for $k_Q^{CS}(t)$[11,18]:

$$k_Q^{CS}(t) = k_\infty[1 + (k_Q^a/k_D)\exp(\chi^2 t)erfc(\chi t^{1/2})] \tag{3.64}$$

where k_∞ is the value of $k_Q^{CS}(t)$ in the long time limit,

$$k_\infty = \lim_{t\to\infty} k_Q^{CS} = k_Q^a k_D/(k_Q^a + k_D) \tag{3.65}$$

and $\chi = [1+(k_Q^a/k_D)]D^{1/2}/\sigma$. With the expression for $k_Q^{CS}(t)$ in Eq. (3.64), the expression for I_o/I in Eq. (3.61) can be evaluated only numerically. For the infinite dilution Stern-Volmer coefficient K_{SV}^o, however, an analytic expression can be derived[18], and found to be identical with Eq. (3.25) if (k_S+F) is replaced by k_S. Deviation of the conventional Smoluchowski theory, Eq. (3.16) along with Eq. (3.64), from the present theory represented by Eq. (3.5) or Eq. (3.23) at higher quencher concentrations will be discussed below through numerical calculation.

Nemzek and Ware[2] derived an approximate expression for I_o/I by using a long time approximation for $k_Q^{CS}(t)$ in evaluating the integral in Eq.(3.61), namely,

$$k_Q^{CS}(t) \cong k_\infty\left[1 + \frac{k_\infty}{k_D}\frac{\sigma}{(\pi Dt)^{1/2}}\right] \tag{3.66}$$

The resulting expression for I_o/I is

$$\frac{I_o}{I} = \frac{1 + C_A^o k_\infty/k_S}{1 - \pi^{1/2}\Omega\exp(\Omega^2)\,erfc(\Omega)} \tag{3.67}$$

where $\Omega = C_A^o k_\infty[k_Q^a/(k_Q^a + k_D)](\sigma^2/\pi D)^{1/2}(k_S + C_A^o k_\infty)^{-1/2}$. As k_Q^a/k_D goes to infinity, Eq. (3.66) for $k_Q^{CS}(t)$ becomes exact and so does Eq. (3.67) for I_o/I. Here, the word "exact" is used only in the scope of the conventional Smoluchowski theory. For Eq. (3.67) to be really exact, the requirement of low light intensity and low quencher concetration should also be met. Nevertheless, Eq. (3.67) is most frequently used

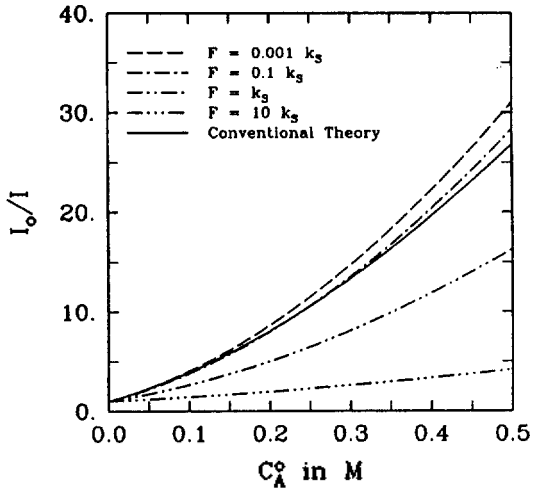

Figure 1. F dependence of the Stern-Volmer plot when $k_Q^o \gg k_D$.

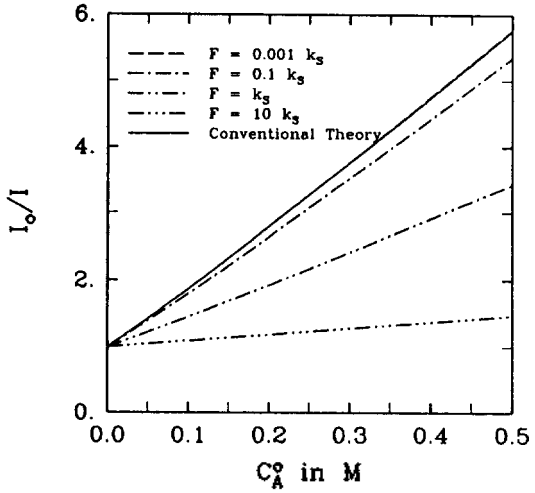

Figure 2. F dependence of the Stern-Volmer plot when $k_Q^o \cong k_D$.

by experimentalists. Expression for K_{SV}^o corresponding to the approximation given by Eq. (3.67) is found to be

$$K_{SV}^o = \frac{1}{k_S}\frac{k_Q^o k_D}{k_Q^o + k_D}\left\{1 + \frac{k_Q^o}{k_Q^o + k_D}\left(\frac{\sigma^2 k_S}{D}\right)^{1/2}\right\} \qquad (3.68)$$

Model Calculations

Eq. (3.5) shows that the relative intensity of quenched to unquenched fluorescence depends on the intensity F of steady illumination, as well as on the quencher concentration C_A^o and other parameters that characterize the diffusive dynamics of the fluorophor and quencher in a given solution. This is an important result since the conventional Smoluchowski approach[11] makes no reference to the probable dependence of I_o/I on F.

Figure 1 shows the F dependence of Stern-Volmer plot. Model parameters used are those for the fluorescence of 1,2-benzanthracene quenched by CBr_4 in 1,2-propanediol at 25°C[2]; $\tau_o = k_S^{-1} = 38.5$ ns, $\sigma = 9.1$ Å, $D = 5.0\times10^{-7}$ cm^2s^{-1} and $k_Q^o = 6\times10^{10}$ $lmol^{-1}s^{-1} = 1\times10^{-10}$ cm^3s^{-1}. In reference 2, Nemzek and Ware evaluated these parameters from an analysis of quenched fluorescence decay data based on the conventional Smoluchowski theory. However, the light pulse used by them to excite fluorophors had a finite width. Thus, their analysis may be erroneous due to the failure of the assumption, made in the conventional theory, that D^* molecules just excited are surrounded by an equilibrium distribution of quencher molecules. In fact, they found[2] that the above parameters deduced from fluorescence decay data are inconsistent with the curvature observed in the Stern-Volmer plots for the same system. Again, their analysis of Stern-Volmer plots was based on the conventional theory. Although we feel that a consistent analysis of the time-dependent and steady-state fluorescence quenching data within the framework of the present theory is desirable, we are not able to carry out the analysis since no information of the intensity of illumination is given in any experimental paper on fluorescence quenching kinetics. For the present, we just take the above values for motional and reaction parameters as the reasonable choice for the input to model calculations to illustrate the implications of the present theory.

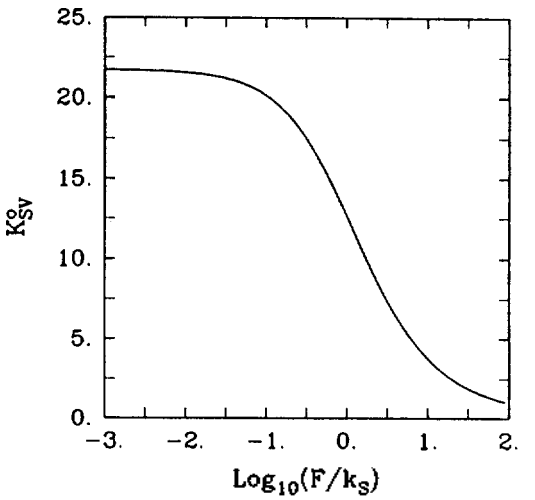

Figure 3. Dependence of the infinite dilution Stern-Volmer coefficient K_{SV}^o on the ratio of F to k_S.

As the light intensity decreases (*i.e.*, $F/k_S \to 0$), the Stern-Volmer curve approaches an asymptote. In Figure 1, this asymptotic curve is almost identical with the dashed curve for the case with $F = 0.001$ k_S. On the other hand, as F increases, the Stern-Volmer curve approaches the horizaontal line, $I_o/I = 1$. Only when $F \ll k_S$ and in the low quencher concentration limit, the conventional Smoluchowski result[11], represented by the solid curve in Figure 1, coincides with the present theory. When compared to the experimental Stern-Volmer plot reported in reference 2, it is seen that the curve predicted by the present theory for the case with $F = 0.001$ k_S shows a little better agreement than the curve predicted by the conventional Smoluchowski theory. However, this observation is merely provisional, since the magnitude of F is unknown and also the parameter values deduced from quenched fluorescence decay data may be inaccurate.

Figure 1 applies to the case when the equilibrium quenching rate constant k_Q^o is much larger than the diffusion-limited rate constant k_D. When k_Q^o is comparable to k_D, we find that the discrepancy between the conventional and pre-

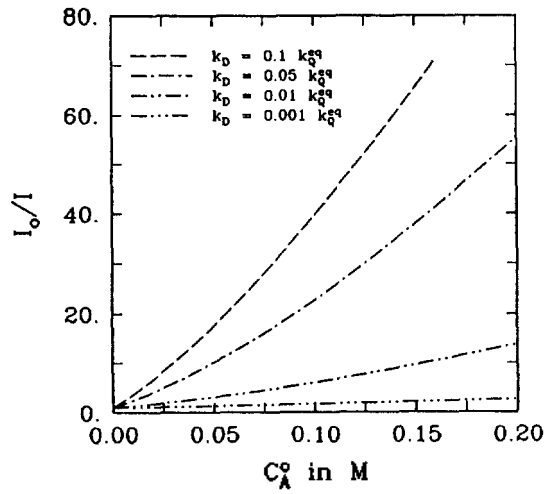

Figure 4. Variation of the Stern-Volmer plot with the ratio of k_D to k_Q^{eq}.

sent theories is not discernible for the whole range of C_A^o as long as the light intensity is kept low. Figure 2 shows this trend. Here, the value of k_Q^{eq} has been set equal to k_D but other parameters are the same as in Figure 1.

In Figure 3, we display the dependence of the infinite dilution Stern-Volmer coefficient K_{SV}^o, as given by Eq. (3.25), on the ratio F/k_S. We have used the same values for the parameters τ_o, σ, D, and k_Q^{eq} as in Figure 1. As F goes to zero, the value of K_{SV}^o approaches a limiting value which coincides with the prediction of the conventional Smoluchowski theory. On the other hand, as F increases K_{SV}^o decreases and eventually becomes unity for very large values of F.

Figure 4 shows that the quenching effect becomes more pronounced as the diffusive encounter rate of D^* and A increases. We used the same values for the parameters τ_o, σ, and k_Q^{eq} as in Figure 1, but changed the value of D such that k_D has the value ranging from 0.001 k_Q^{eq} to 0.1 k_Q^{eq}. We fixed the value of F at 0.001 k_S.

Figure 5 displays the effect of an attractive Coulomb force on the quenching dynamics. Except that the potential of mean force $U(r)$ is now given by

$$U(r)=k_BT(r_c/r) \quad \text{for } r>\sigma \tag{4.1}$$

with $r_c=Z_AZ_De^2/\varepsilon k_BT=-5.0$ Å (Z_Ae and Z_De are charges on A and D molecules, respectively, and ε is the dielectric constant of the solvent), other parameters have the same values as in Figure 1. In Figure 5(a) $F=0.001\ k_S$, while in Figure 5(b) $F=k_S$. The solid curves are exact results obtained by solving Eqs. (3.1)-(3.3) numerically. Approximate analytic results based on Eq. (3.43) are represented by dot-dashed curves, which can be hardly distinguished from the exact results. The "effective-radius" results, represented by the dashed curves, were calculated from the potential-free equation for I_o/I [*i.e., Eq. (3.23)*] but with the contanct radius σ replaced by an effective value for the reaction radius[11]:

$$\sigma_{eff}=r_c[(1+4\pi r_cD/k_Q^{eq})\exp(r_c/\sigma)-1]^{-1} \tag{4.2}$$

As expected, the attractive force between A and D^* molecules amplifies the quenching effect. An opposite effect is found for the repulsive interaction.

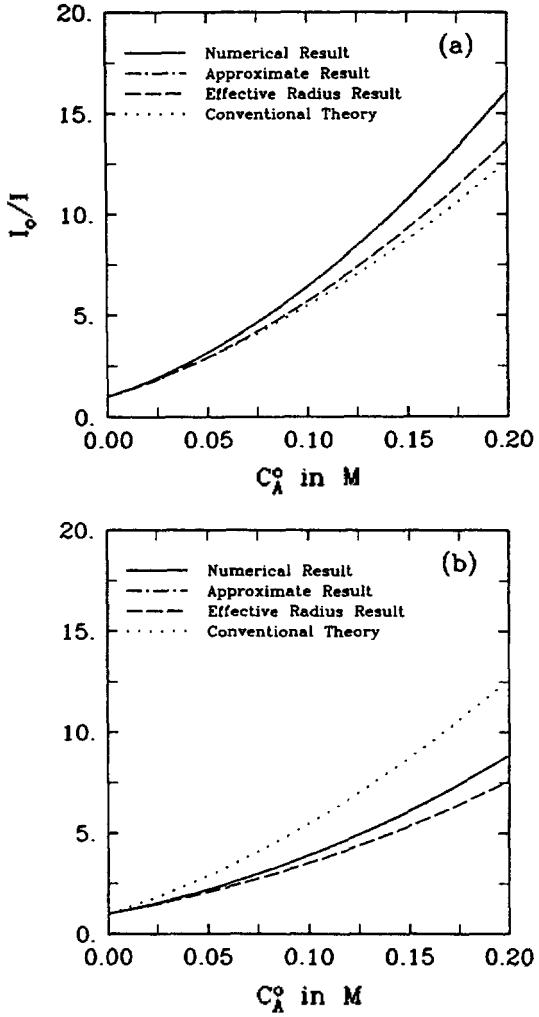

Figure 5. Effects of an attractive Coulomb potential on the Stern-Volmer plot. $F=0.001\ k_S$ for Figure 5(a) and $F=k_S$ for Figure 5(b).

Effects of long-range energy transfer are shown in Figures 6(a) and 6(b). We assume that the long-range energy transfer occurs *via* the dipole-dipole interaction mechanism[24] so that $S_L(r)$ in Eq. (3.44) is given by

$$S_L(r)=\tau_o^{-1}(R_o/r)^6 \tag{4.3}$$

where R_o is the critical separation for which energy transfer from D^* to A and unimolecular decary of D^* are equally probable. We set the value of R_o equal to 20 Å. Again, we assumed that $U(r)=0$ for $r>\sigma$ and other parameters used are the smae as in Figure 1. In Figure 6(a) $F=0.001\ k_S$, while in Figure 6(b) $F=k_S$. The solid curves are exact results obtained by solving Eqs. (3.1)-(3.3) numerically. Approximate analytic results based on Eq. (3.60) are represented by dot-dashed curves, which deviate much from the exact results. However, the "effective-radius" results, which were calculated from Eq. (3.23) but with the contact radius σ replaced by an effective reaction radius σ_{eff}[11],

$$\sigma_{eff}=R_o\frac{(R_o^2/D\tau_o)^{1/4}\Gamma(3/4)}{2\Gamma(5/4)}\left[1+(2^{1/2}/\pi)\cdot\frac{K_{1/4}(z_o)}{I_{1/4}(z_o)}\right] \tag{4.4}$$

$$\cong 0.676(R_o^2/D\tau_o)^{1/4}R_o\{1+1.414\exp[-R_o^3/(D\tau_o)^{1/2}\sigma^{-2}]\}$$

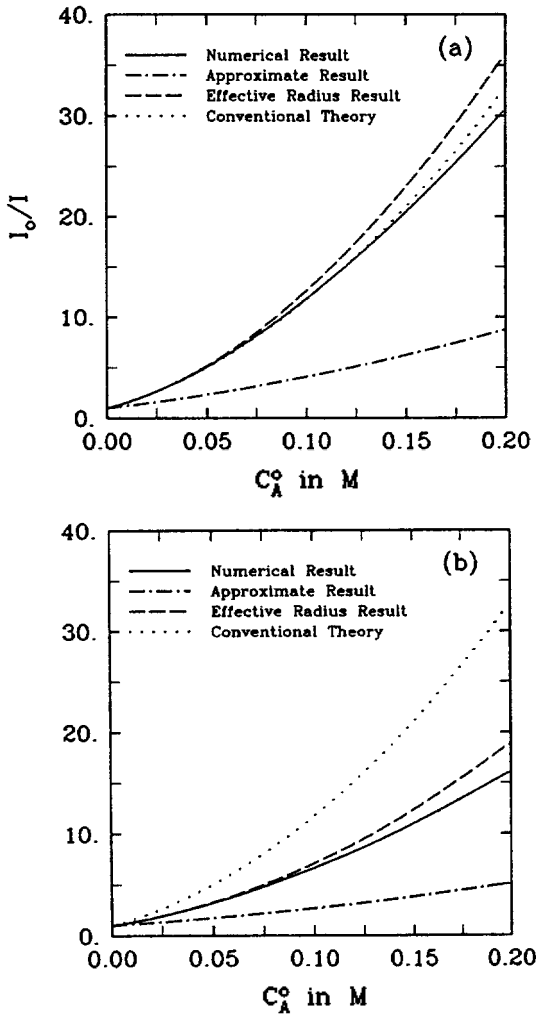

Figure 6. Effects of a long-range energy transfer on the Stern-Volmer plot. $F=0.001\ k_S$ for Figure 6(a) and $F=k_S$ for Figure 6(b).

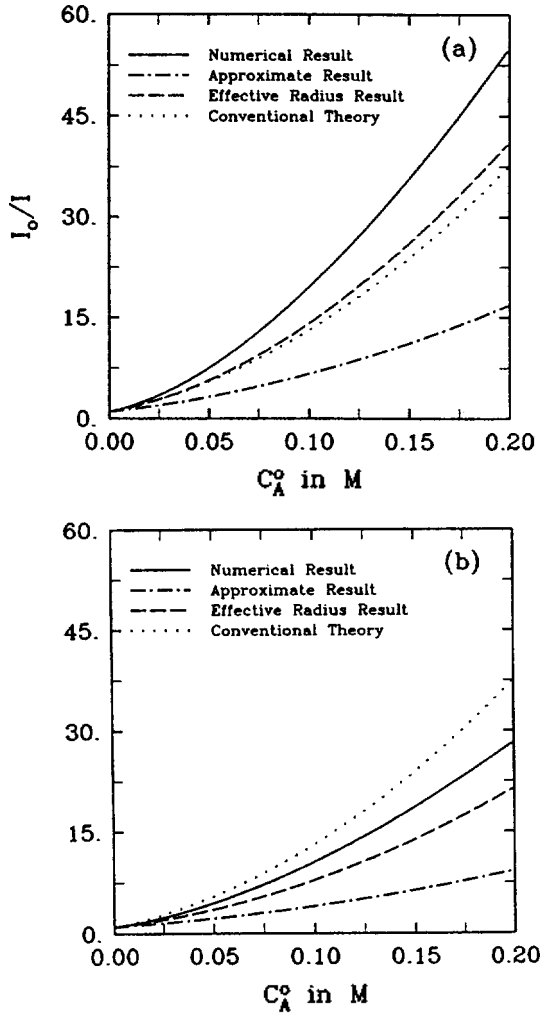

Figure 7. Combined effects of an attractive Coulomb potential and a long-range energy transfer on the Stern-Volmer plot. $F=0.001\ k_S$ for Figure 7(a) and $F=k_S$ for Figure 7(b).

are again in relatively good agreement with the exact results. Here, $z_o=(1/2)(R_o^6/D\tau_o)^{1/2}\sigma^{-2}$, $\Gamma(z)$ is the gamma function, and $K_\nu(z)$ and $I_\nu(z)$ are the modified Bessel functions of order ν[25]. It can be seen that the additional long-range energy transfer increases the quenching effect.

Finally, the combined effects of long-range energy transfer and attractive Coulomb potential are displayed in Figures 7(a) and 7(b). The long-range sink function $S_L(r)$ is again assumed to be given by Eq. (4.3) with $R_o=20$ Å, and the Coulomb potential is given by Eq. (4.1) with $r_c=-5.0$ Å. All other parameters have the same values as in Figure 1. In Figure 7(a) $F=0.001\ k_S$, while in Figure 7(b) $F=k_S$. Again, approximate analytic results based on Eq. (3.60) deviate much from the exact numerical results. Even the "effective-radius" results calculated from Eq. (3.23) with σ_{eff} given by

$$\sigma_{eff}=r_c[(1+4\pi r_c D/k_Q^o)\exp(r_c/\sigma'_{eff})-1]^{-1};$$
$$\sigma'_{eff}=0.676(R_o^2/D\tau_o)^{1/4}R_o\{1+1.414\exp[-R_o^3/(D\tau_o)^{1/2}\sigma^{-2}]\} \quad (4.5)$$

are not in good agreement with the exact results.

Concluding Remarks

We have applied the theory developed in a previous work[20] to investigate the effects of potential of mean force and long-range energy transfer processes. The present theory predicts a rather complicated nonlinear dependence of I_o/I (the relative intensity of unquenched to quenched fluorescence) on the quencher concentration C_A^o. Effects of the potential of mean force on the quenching dynamics are evaluated to a good accuracy by an approximate analytic equation, namely, by Eq. (3.43). However, the approximate analytic formula for evaluating the effects of long-range energy transfer processes, given by Eq. (3.60), appears less helpful. Instead, *ad hoc* approximations, based on what we call "effective-radius" formulas, Eqs. (4.4) and (4.5), offer more accurate estimations. Since even the full numerical calculation that solves Eqs. (3.1)-(3.3) directly is found to be not too demanding, it is recommended in preference to either of the approximate analytic procedures when the effects of long-range energy transfer are to be evaluated. An important aspect of the present theory is that it describes the dependence of fluorescence quenching dynamics on the intensity of external illu-

mination. The conventional Smoluchowski approaches[11] are mute in this respect; it has been simply assumed that the intensity of illumination should be quite weak. Hence the validity of the present theory may be tested by a fluorescence quenching experiment under intense illumination.

Acknowledgement. This work was supported by a grant from the Basic Science Research Program, Ministry of Education of Korea, 1989.

References

1. J. B. Birks, Photophysics of aromatic molecules (Wiley, New York, 1970).
2. T. L. Nemzek and W. R. Ware, *J. Chem. Phys.*, **62**, 477 (1975).
3. D. P. Millar, R. J. Robbins, and A. H. Zewail, *J. Chem. Phys.*, **75**, 3649 (1981).
4. R. W. Wijnaendts van Resandt, *Chem. Phys. Letters.*, **95**, 205 (1983).
5. N. Tamai, T. Yamazaki, I. Yamazaki, and N. Mataga, *Chem. Phys. Letters.*, **120**, 24 (1985).
6. J. R. Lakowicz, M. L. Johnson, I. Gryczynski, N. Joshi, and G. Laczko, *J. Phys. Chem.*, **91**, 3277 (1987).
7. N. Periasamy, S. Doraiswamy, B. Venkataraman, and G. R. Fleming, *J. Phys. Chem.*, **89**, 4799 (1988).
8. G. C. Joshi, R. Bhatnagar, S. Doraiswamy, and N. Periasamy, *J. Phys. Chem.*, **94**, 2908 (1990).
9. F. Heisel and J. A. Miehe, *J. Chem. Phys.*, **77**, 2558 (1982).
10. J. K. Baird and S. P. Escott, *J. Chem. Phys.*, **74**, 6993 (1981).
11. S. A. Rice, Diffusion-limited reactions in comprehensive chemical kinetics, Vol. 25, eds., C. H. Bamford, C. F. H. Tipper, and R. G. Compton (Elsevier, Amsterdam, 1985).
12. G. Wilemski and M. Fixman, *J. Chem. Phys.*, **58**, 4009 (1973).
13. U. Gösele, M. Hauser, U. K. A. Klein, and R. Frey, *Chem. Phys. Letters.*, **34**, 519 (1975).
14. J. K. Baird, J. S. McCaskill, and N. H. March, *J. Chem. Phys.*, **74**, 6812 (1981).
15. R. I. Cukier, *J. Chem. Phys.*, **82**, 5457 (1985).
16. B. Stevens, *Chem. Phys. Letters.*, **134**, 519 (1987).
17. J. Najbar, *Chem. Phys.*, **120**, 367 (1988).
18. A. Szabo, *J. Phys. Chem.*, **93**, 6929 (1989).
19. H. Zhou and A. Szabo, *J. Chem. Phys.*, **92**, 3874 (1990).
20. S. Lee, M. Yang, K. J. Shin, K. Y. Choo, and D. Lee, *Chem. Phys.*, In press.
21. S. Lee and M. Karplus, *J. Chem. Phys.*, **86**, 1883 (1987).
22. S. Lee, Ph. D. Thesis, Harvard University (1986).
23. P. Sibani and J. B. Pedersen, *J. Chem Phys.*, **74**, 6934 (1981).
24. T. Förster, *Ann. Phys.*, **2**, 55 (1948).
25. M. Abramowitz and I. A. Stegun, Handbook of mathematical function (Dover, New York, 1970).

Memory of Initial States in Scattering over Attractive Potential Energy Surface for Atom-Diatom Collisions

Seung-Ho Choi and Hyung-Rae Kim*

Department of Chemistry, Hankuk University of Foreign Studies, Seoul 449-791.

Received March 22, 1991

Global and local momory functions, defined by Quack and Troe, were calculated for the rotationally inelastic collision of $O+SO(v, j)\rightarrow[O\text{--}S\text{--}O]\rightarrow O+SO(v, j')$. It is seen to decrease steadily as total energy increases. Distribution of scattering cross section over product rotational states also shows the decreasing memory of initial state as total energy is increased. These results are interpreted in terms of energy scrambling at high energy due to the availability of more phase space and also the influence of strong dynamical constraints.

Introduction

It is possible to calculate detailed state-to-state scattering cross sections for the reactions involving strongly coupled intermediate collision complexes using several well-formulated statistical theoreis[1,2] and the product state distributions for these kinds of collisions can be predicted reasonably well for some cases. Such complexes can be formed only over a deep potential well. Many neutral atom-diatom collisions are direct in nature. However a bimolecular reaction between two radical fragments of a stable triatomic molecule is known to proceed through intermediate collision complex[3,4], which is none other than highly vibrationally excited (over the dissociation limit) triatomic molecule. Therefore it would be very useful for the understanding of the reaction dynamics of a system involving the strong coupled collision complex if one could interpret the product state distribution in terms of the degree to which the initial states retain the momory of initial quantum states. This memory is closely related to the problem of redistribution of internal energy initially acquired in specific degrees of freedom[5]. The product state distribution, which is usually what is observed experimentally, can be related to the degree of ergodic state mixing that happens extensively in the strong coupling region of the complex.[6].

Even though the actual dynamics of the complex collision